

Propagation of Transient Signals in a Magnetoactive Plasma

MAHMOUD OMID and MASASHI HAYAKAWA

Dept. of Electrical Engineering, The University of Electro-communications
1-5-1 Chofugaoka, Chofu Tokyo 182, Japan

1. Introduction

The transient propagation of electromagnetic pulses in a magnetoactive plasma has been of interest for diagnostic purposes. One of the most popular approaches in studying pulse propagation in the plasma is to obtain an approximate analytical expression for the wave packet by using the saddle-point method of integration(Vidmar *et al.*[1];Felsen and Marcuvitz[2]). In a previous study by Ishimaru[3] the transient excitation by a current source in a lossless magnetoactive plasma was formulated, but no numerical results were presented. Recently,Vidmar *et al.* have given some numerical results on the transient excitation of delta function current source in the ionospheric F₂ layer on the assumption that the observation point is located many wavelengths from the source by using the saddle-point approximation.

In this paper, we extend Ishimaru's formulation to a more general case of two-component lossy magnetoplasma, and then use a numerical inversion method of the Laplace transform(Hosono[4]) to evaluate the exact transient field components.

2. General Formulation

Cartesian coordinates are used with the z axis, parallel to the static magnetic field **B**₀, which is assumed to be the direction of propagation. It is well known that a magneto-ionic medium can support two independent circularly polarized waves[3,5]. However, it is shown that the time-domain formulation must consist of a proper combination of the two waves if we are to obtain a *casual, real-time* transient solution in the final expression[3]. In order to assure these criteria, the correct formulation should be of the form

$$\mathbf{E}(z, t) = \frac{1}{2\pi j} \int_{Br} [\tilde{\mathbf{C}}_R(s)e^{-s\mathbf{n}_R z/c} + \tilde{\mathbf{C}}_L(s)e^{-s\mathbf{n}_L z/c}]e^{st} ds \quad (1)$$

$$\mathbf{n}_R = \left(1 + \frac{\omega_{pe}^2}{s(s - j\omega_{ce})} \right)^{\frac{1}{2}} \Bigg|_{s=j\omega}, \quad \mathbf{n}_L = \left(1 + \frac{\omega_{pe}^2}{s(s + j\omega_{ce})} \right)^{\frac{1}{2}} \Bigg|_{s=j\omega}, \quad \tilde{\mathbf{C}}_L(s) = \tilde{\mathbf{C}}_R^*(s^*)$$

where * denotes a complex conjugate and Br defines a Bromwich path in the complex s-plane (s = jω). ω_{pe}, ω_{ce} are the angular electron plasma and cyclotron frequencies, respectively. Coefficients $\tilde{\mathbf{C}}_R(s)$ and $\tilde{\mathbf{C}}_L(s)$ are functions of the source excitation and can be obtained using a standard procedure[1,3]. \mathbf{n}_R and \mathbf{n}_L are the refractive indices of the right- and left- handed circularly polarized waves which are functions of s. Using s = jω, then for a two-component plasma consisting of electrons and one ion species, we have

$$\mathbf{n}_R^2 = 1 + \frac{1}{s(s + Z_e)} + \frac{W_i^2}{s(s + Z_i^*)}, \quad \mathbf{n}_L(s) = \mathbf{n}_R^*(s^*) \quad (2)$$

where, $s = \frac{j\omega}{\omega_{pe}}$, $Z_e = V_e - jW_{ce}$, $Z_i = V_i - jW_{ci}$, $V_e = \frac{\nu_e}{\omega_{pe}}$, $V_i = \frac{\nu_i}{\omega_{pi}}$, $W_{ce} = \frac{\omega_{ce}}{\omega_{pe}}$, $W_{ci} = \frac{\omega_{ci}}{\omega_{pe}}$, $W_i = \frac{\omega_{pi}}{\omega_{pe}}$. ω_{pi}, ω_{ci} are the angular ion plasma and cyclotron frequencies; ν_e, ν_i are the collision frequencies of electrons and ions, respectively.

3. The Excitation of Waves in a Magnetoactive plasma by a Current Source

The excitation of waves in a magneto-ionic medium by a delta function current source is depicted in Fig.1, where the current source is represented by $\mathbf{J}_x(z, t)$ and $\mathbf{J}_y(z, t)$. The transform solution relating the electric field $\mathbf{E}(z, t)$ and the source current $\mathbf{J}(z, t)$, assuming no variation in x and y , is found by integrating over the k -plane [3]

$$\tilde{\mathbf{E}}_x(s, k) = -\frac{c\mu_0}{4} \left[\frac{\tilde{\mathbf{J}}_x(s, k) - j\tilde{\mathbf{J}}_y(s, k)}{\mathbf{n}_R} e^{-s\mathbf{n}_R z/c} + \frac{\tilde{\mathbf{J}}_x(s, k) + j\tilde{\mathbf{J}}_y(s, k)}{\mathbf{n}_L} e^{-s\mathbf{n}_L z/c} \right] \quad (3)$$

$$\tilde{\mathbf{E}}_y(s, k) = -\frac{c\mu_0}{4} \left[j \frac{\tilde{\mathbf{J}}_x(s, k) - j\tilde{\mathbf{J}}_y(s, k)}{\mathbf{n}_R} e^{-s\mathbf{n}_R z/c} - j \frac{\tilde{\mathbf{J}}_x(s, k) + j\tilde{\mathbf{J}}_y(s, k)}{\mathbf{n}_L} e^{-s\mathbf{n}_L z/c} \right] \quad (4)$$

The time-dependent field components $\mathbf{E}_x(z, t)$ and $\mathbf{E}_y(z, t)$ for the wave packet propagating with $z > 0$ are then given by

$$\mathbf{E}_x(z, t) = \frac{1}{2\pi j} \int_{B_r} \tilde{\mathbf{E}}_x(k, s) e^{st} ds, \quad \mathbf{E}_y(z, t) = \frac{1}{2\pi j} \int_{B_r} \tilde{\mathbf{E}}_y(k, s) e^{st} ds \quad (5)$$

Using the symmetry property of Eq.(2), this can be written as

$$\mathbf{E}_x(z, t) = \frac{1}{2\pi j} \int_{B_r} \tilde{\mathbf{C}}_R(s) e^{s(t - \mathbf{n}_R z/c)} ds + c.c. \quad (6)$$

$$\mathbf{E}_y(z, t) = \frac{1}{2\pi j} \int_{B_r} j \tilde{\mathbf{C}}_R(s) e^{s(t - \mathbf{n}_R z/c)} ds + c.c. \quad (7)$$

with $\tilde{\mathbf{C}}_R(s) = -\frac{c\mu_0(\tilde{\mathbf{J}}_x(s, k) - j\tilde{\mathbf{J}}_y(s, k))}{4\mathbf{n}_R}$, where *c.c.* denotes the complex conjugate of the first integral on the right-hand side of Eqs.(6) and (7) and is zero for a current source, such that $\mathbf{J}_x(s, k) = -j\mathbf{J}_y(s, k)$. In general, the polarization between $\mathbf{E}_x(z, t)$ and $\mathbf{E}_y(z, t)$ is not circular. Note these integrals cannot be evaluated in a closed form. But, since $\tilde{\mathbf{C}}_R(s)$ is well behaved for real s , a numerical solution is possible. Next we define the excitation pulse as

$$\mathbf{J}_x(t, z) = J_1 \delta(t) \delta(z) \longleftrightarrow \tilde{\mathbf{J}}_x(s, k) = J_1, \quad \mathbf{J}_y(t, z) = J_2 \delta(t) \delta(z) \longleftrightarrow \tilde{\mathbf{J}}_y(s, k) = J_2 \quad (8)$$

where $\delta(t)$ and $\delta(z)$ are the temporal and spatial delta functions. J_1 and J_2 are dimensional constants. The role of $\delta(z)$ is to confine the current source to a sheet in the z plane. For the propagation parallel to the magnetic field, excitation currents, $\mathbf{J}_x(s, k)$ and $\mathbf{J}_y(s, k)$ are equivalent and produce similar waveforms.

4. Numerical Results and Discussion

The transient field components $\mathbf{E}_x(z, t)$ and $\mathbf{E}_y(z, t)$ were evaluated by using the numerical inversion method of the Laplace transform which is proposed in [4]

$$f(t) \triangleq L^{-1}[F(s)] = \frac{e^a}{t} \left(\sum_{n=1}^{2k} (-1)^n F_n + \frac{1}{2^p} \sum_{q=1}^p (-1)^{q-1} A_{p,q} F_{2k+q} \right) \quad (9)$$

where $F_n \triangleq \text{Im}\{F(a/t + j[n - 0.5]\pi/t)\}$, $A_{pq} = 1$, $A_{p,q-1} = A_{pq} + p C_{q+1}$; a : approximation parameter; k, p : the number of truncation and Euler transformation terms. Here, we carried

Table.1 Ionospheric parameters

parameter	value, normalized with ω_{pe}
ω_{pe}	$2\pi \times 10^7 \text{ sec}^{-1}$
ω_{pi}	$5.83 \times 10^{-3} \omega_{pe}$
ω_{ce}	$0.10 \omega_{pe}$
ω_{ci}	$3.4 \times 10^{-6} \omega_{pe}$
ω_R	$1.055 \omega_{pe}$
ω_L	$.955 \omega_{pe}$
ν_e	$1.59 \times 10^{-5} \omega_{pe}$
ν_i	$5.41 \times 10^{-10} \omega_{pe}$

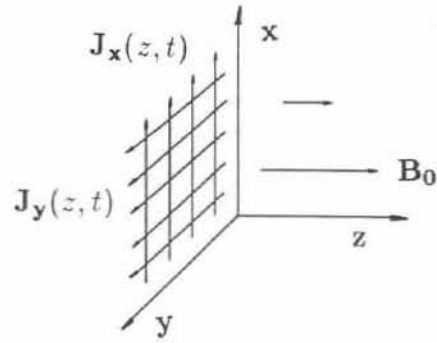


Fig.1 Orientation of the delta function current source, $J_x(z, t)$ and $J_y(z, t)$, with $t=0$

out numerical computation using parameters which make the relative error less than 10^{-5} .

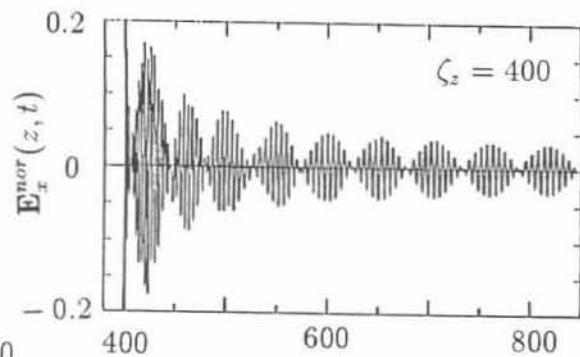
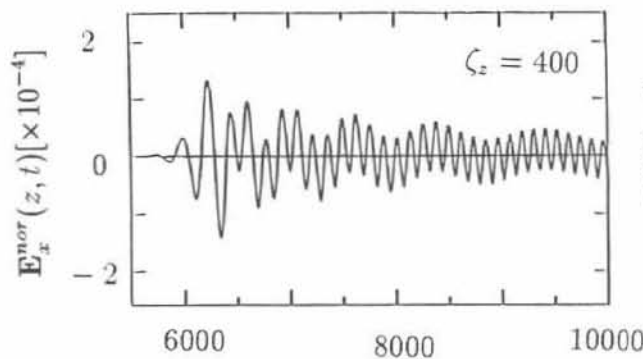
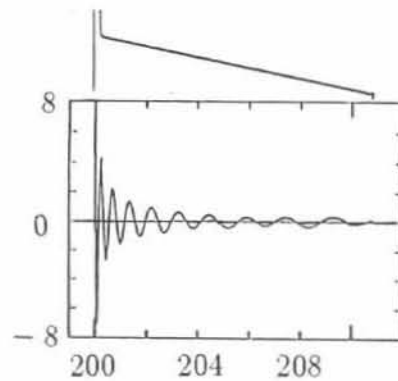
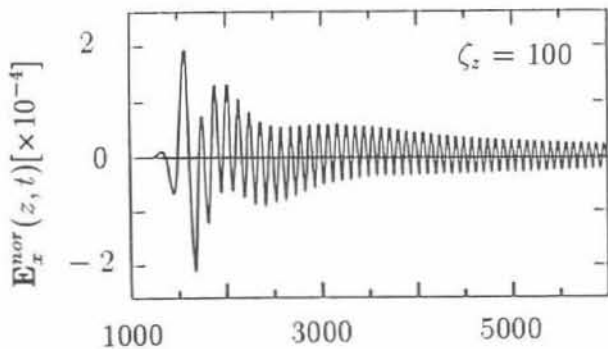
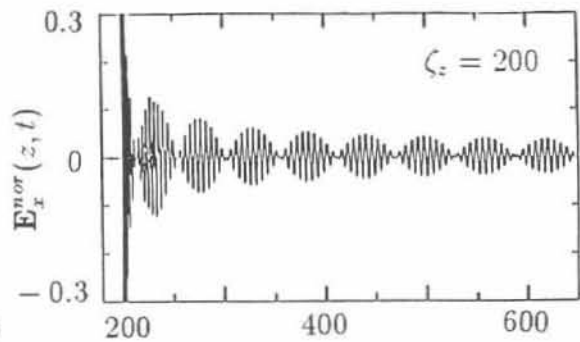
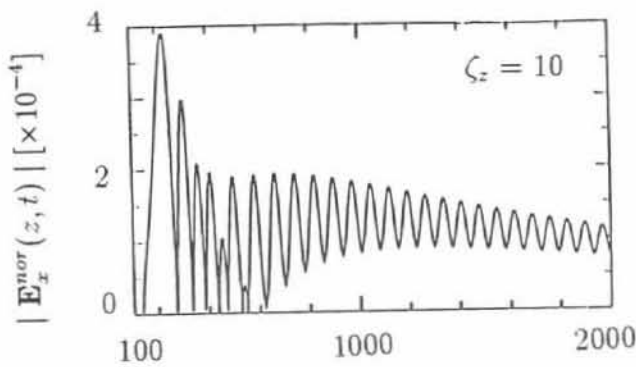
To permit comparison with Ref.[1], we set $J_2 = 0$, and use the daytime F_2 layer ionospheric parameters as given in Table 1, where ω_R and ω_L are the cut-off frequencies of the right- and left-handed circularly polarized waves, respectively. The results are illustrated in Figs.2 and 3. In these figures $\tau = \omega_{pe} t$, $\mathbf{E}_x^{nor}(z, t) (= -\frac{4\mathbf{E}_x(z, t)}{\omega_{pe}\mu_0 J_1})$ is the normalized electric field and $\zeta_z (= \frac{\omega_{pe} z}{c})$ is dimensionless distance from the interface.

Fig.2 illustrates the waveforms for the whistler branch at $\zeta_z = 10, 100$ and 400 . The initial part of $\zeta_z = 10$ plot is a whistler branch precursor. The rapid increases in amplitude for $\zeta_z = 100$ and $\zeta_z = 400$ plots are closely related to the wave components with frequencies near $\omega_{ce}/4$ because the group velocity at $\omega_{ce}/4$ attains its maximum value in the case of a homogeneous magnetoplasma. The subsequent modulation envelopes are resulted from the interference between the wave components above and below $\omega_{ce}/4$. The wave components with $\omega > \omega_{ce}/4$ decay more quickly due to the collisional damping than those at $\omega < \omega_{ce}/4$. Nevertheless the the envelope modulation becomes more enhanced at larger distances ($\zeta_z = 400$). This is due to stronger interference caused by the waves in the narrow band just around $\omega = \omega_{ce}/4$.

Fig.3 shows the waveforms for the high frequency branch (*i.e.* quasi-free space mode waves at $\omega > \omega_{pe}$). In this range there are two possible modes of propagation (right- and left-handed waves). The figures with $\zeta_z = 200$ and 400 illustrate the progressive decomposition of the spike into its frequency components. This decomposition becomes more enhanced at increased ζ_z because small differences in group velocity over greater distances might result in the broadening of the spike. Then, the observed conspicuous modulation envelope is resulted from the interference between the wave components in the right- and left-handed polarized waves. Near the cutoff frequencies of these branches at ω_R and ω_L , wave components with identical group velocities ($v_g \rightarrow 0$) have frequencies which differ by $\omega_R - \omega_L \simeq \omega_{ce}$ and produce a modulation envelope with frequency $\omega_{ce}/2$.

5. Conclusion

Only a few examples are given here because of limited available space, but it obvious that the approach mentioned above will open a new methodology for different areas and is an alternative and simple method to long-existing methods[1][2].



TIME, τ

Fig.2 Whistler waveforms for $\mathbf{k} \parallel \mathbf{B}_0$, with $\tilde{\mathbf{J}}_x(s, k) = J_1$ and $\tilde{\mathbf{J}}_y(s, k) = 0$

TIME, τ

Fig.3. High frequency waveforms for $\mathbf{k} \parallel \mathbf{B}_0$, with an expanded time scale

The numerical inverse Laplace transform adopted in this paper has the following advantages over the previous saddle point method; (1) It is an exact solution to the problem valid for any plasma parameters, and also even at the initial arrival of the pulse, (2) Any linear dispersion relation may be used, (3) Computation time is moderate, and (4) Similar approaches can be utilized in different areas including transient propagation of waves with different initial waveforms such as lightning, Gaussian envelope carrier pulse *etc.*

6. References

- [1] Vidmar R. J. *et al.* (1983). *Radio Science*, **18**, pp.1337-1354.
- [2] Felsen L. B. and N. Marcuvitz (1973). *Radiation and Scattering of Waves*, pp.370-441.
- [3] Ishimaru A. (1967). *Electromagnetic Wave Theory*, Vol.2, Ed. J. Brown, pp.125-134.
- [4] Hosono T. (1981). *Radio Science*, **16**, pp.1015-1019.
- [5] Budden K. G. (1961). *Radio Waves in the Ionosphere*, Section 5.3.